DFT/TDDFT study of the adsorption of N3 and N719 dyes on ZnO(10$\bar{1}$0) surfaces

ARTICLE *in* THE JOURNAL OF PHYSICAL CHEMISTRY A · APRIL 2014

Impact Factor: 2.69 · DOI: 10.1021/jp501058x · Source: PubMed

2 AUTHORS:

Jon Mikel Azpiroz
Italian National Research Council
21 PUBLICATIONS **142** CITATIONS
SEE PROFILE

Filippo De Angelis
Università degli Studi di Perugia
264 PUBLICATIONS **11,206** CITATIONS
SEE PROFILE

THE JOURNAL OF PHYSICAL CHEMISTRY A

Article

pubs.acs.org/JPCA

DFT/TDDFT Study of the Adsorption of N3 and N719 Dyes on ZnO(10$\bar{1}$0) Surfaces

Jon M. Azpiroz[†] and Filippo De Angelis*[,‡]

[†]Kimika Fakultatea, Euskal Herriko Unibertsitatea (UPV/EHU) and Donostia International Physics Center (DIPC), P. K. 1072, 20080 Donostia, Euskadi, Spain

[‡]Computational Laboratory for Hybrid/Organic Photovoltaics (CLHYO), Istituto CNR di Scienze e Tecnologie Molecolari (ISTM-CNR), Via Elce di Sotto 8, 06123 Perugia, Italy

Supporting Information

ABSTRACT: ZnO has attracted a great deal of research as a potential replacement of TiO_2 for dye-sensitized solar cells (DSSCs), owing to the unique combination of interesting electronic properties (i.e., high electron mobility) and structural richness. Here, we present a DFT/TDDFT study about the interaction of the prototypical N3 and N719 Ru(II) sensitizers on ZnO models to understand some of the atomistic details that are crucial to the dye/semiconductor interaction. We pay particular attention to the adsorption mode of the sensitizer and to the effect of the complexation on the electronic structure of the dye. The sensitizers are predicted to strongly interact with the ZnO surface. In particular, the interaction is strengthened when three dye carboxylic groups are involved in the adsorption. Moreover, if the anchoring group bears a proton, the adsorption is predicted to be dissociative. The charge density donation from the dye to the semiconductor raises the valence and conduction band edges of the latter, in such a way that the optical gap of ZnO widens. Proton transfer from the dye to the semiconductor balances the charge donation effect and restores the electronic levels of the noninteracting fragments. The impact of dye/semiconductor interaction on the adsorbed dye optical properties is then discussed.

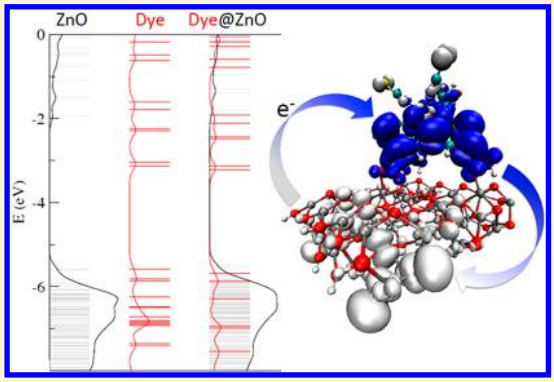

1. INTRODUCTION

Over the last decades, the depletion of fossil fuels and the serious environmental concerns associated with their combustion have triggered the development of new energy sources. In particular, solar energy emerged as a clean, efficient, renewable, and sustainable alternative. The dye-sensitized solar cells (DSSCs) first developed by O'Regan and Grätzel represented a key breakthrough for the efficient light conversion at low cost.[1] DSSCs consist of a mesoporous wide-gap semiconductor layer, typically TiO_2, grafted with a monolayer of sensitizing dye, which absorbs solar radiation and injects the photoexcited electrons into the conduction band of the semiconductor.[2] The concomitant hole is then usually trasferred to a redox shuttle, closing the circuit.

Ruthenium(II) polypyridyl complexes are among the most popular light harvesters within the solar cell community. In particular, the prototype [*cis*-(dithiocyanato)-Ru-bis(2,2′-bipyridine-4,4′-dicarboxylate)] complex (N3) and its doubly protonated tetrabutylammonium salt (N719) have maintained a clear lead due to their efficiency.[3,4] In this type of compounds, the bipyridine ligands ensure stable anchoring to the semiconductor surface through the carboxylic groups, allowing for the strong electronic coupling required for efficient excited-state electron injection. On the other hand, the thiocyanate ligands guarantee fast regeneration of the oxidized dye.[5]

Regarding the semiconductor, TiO_2 is probably the most widely employed compound in DSSC devices. However, a significant deal of research is being devoted to other other metal oxides such as SnO_2, ZnO, Nb_2O_5, and WO_3.[6−11] SnO_2 and ZnO are particularly interesting materials because the electron mobility in their bulk phases is over 2 orders of magnitude higher than that of TiO_2.[6,12−15] As a consequence, the charge recombination losses should be minimized in SnO_2- and ZnO-based DSSCs. Moreover, ZnO is particularly amenable for DSSCs because it possesses virtually identical band energetics as TiO_2 in their bulk form.[6−10] Furthermore, ZnO has been reported to crystallize in a plethora of nanometric shapes, ranging from nanorods and nanowires to tetrapods,[16,17] depending on the experimental conditions. Such structural richness has received considerable interest because it introduces a new variable for the on-purpose modification of the electronic properties of the DSSC photoanode. Elongated nanostructures are particularly attractive for photovoltaic applications because they offer a directional charge carrier

Special Issue: Energetics and Dynamics of Molecules, Solids, and Surfaces - QUITEL 2012

Received: March 26, 2014
Published: April 10, 2014

pathway toward electrodes and prevent recombination events during transport across the semiconductor.[18]

Despite their paramount technological potential, ZnO-based devices have performed quite disappointingly so far, with record efficiencies of ∼8%,[19] whereas for TiO_2, DSSC efficiencies exceeding 12% have been reported.[20] The reasons underlying this efficiency gap remain unclear. The electronic structure of the semiconductor might play a role because bulk ZnO and TiO_2 possess similar band gaps and conduction band energies but a quite different band structure. In particular, ZnO shows a much smaller density of states than TiO_2 at the edge of the conduction band, making the electron injection from the dye excited state less favorable.[21,22] Moreover, the lowest-lying unoccupied states of TiO_2 arise from Ti 3d t_{2g} orbitals, whereas the conduction band edge (CBE) of ZnO is comprised primarily of Zn 4s states. As a consequence, different coupling with the excited dye states can be anticipated.

Besides, when approaching the nanoscale, quantum confinement effects are known to largely influence the band edges of ZnO.[23−25] With the decreasing structure size, the conduction band experiences a significant upward shift, and the probability of electron injection from the photoexcited dye decreases.[26] On the contrary, the band edge states and the band gap of TiO_2 appear to be quite insensitive to particle size above a minimum threshold.[22] Moreover, nanostructures often develop midgap states that could act as traps for the photogenerated electrons, thus lowering the performance of the device. ZnO nanostructures in particular are known to bear a dense distribution of intraband defect states.[6,27] Therefore, even if bulk ZnO produces better transport of charge carriers than TiO_2, in current DSSC nanocomposites, both metal oxides perform basically the same because charge diffusion is limited by electronic trap states.[28]

The performance of DSSCs is not determined solely by the semiconductor nature, but the interface with the sensitizer plays a pivotal role. Electron injection from the photoexcited dye is a complex process, and a great deal of research is being devoted to its understanding. For the typical sensitizers effectively used with TiO_2, slow electron injection rates have been found for ZnO,[29] presumably due to the formation of interface-bound charge-separate pairs, which play the role of intermediate states prior to generation of free electrons.[30−32] These long-lived pairs, not found for TiO_2, have been ascribed to the low dielectric constant of ZnO (∼8 versus ∼30−170 for TiO_2[33]).

From a different perspective, the chemical interaction between the dye and the semiconductor is also very important. In this respect, the interface between different sensitizers and TiO_2 has been investigated thoroughly. Prototypical dyes bearing carboxylic groups seem to be unsuitable to ZnO sensitization due to the poor chemical stability of ZnO electrodes in the presence of acids, with the concomitant release of Zn^{2+} ions.[34] Dyes containing complexing groups could also remove Zn^{2+} from the ZnO lattice.[35] As a consequence, dye/Zn complexes are often formed in ZnO DSSCs, resulting in a poor performance of the device. To circumvent this drawback, other dyes are being checked. Indoline sensitizers, in particular, have been successfully tested.[36] The lower interaction with ZnO surfaces prevents the complex formation, but it also gives rise a weak and unstable sensitization effect.

Computational simulations rooted in density functional theory (DFT) and time-dependent DFT (TDDFT) have become a crucial tool to understand the detailed atomistic features governing the performance of TiO_2 DSSCs.[2,3,5,37−41] Studies on dye-sensitized ZnO models are however scarce (see, for example, refs 42−47), and to the best of our knowledge, the interaction of the prototypical N3/N719 Ru(II) dyes with ZnO has never been reported. In order to fill this void, here we present a DFT/TDDFT study about the interaction between the prototypical dyes N3/N719 and a model ZnO nanostructure. We pay particular attention to the adsorption modes, geometries, and energies. The role of the proton transfer from the dye to the semiconductor surface is also tested. Besides, we study the effect of interaction on the electronic and optical properties of the dye and the semiconductor.

2. COMPUTATIONAL DETAILS

Figure 1 depicts the optimized geometries of the semiconductor and dye models employed throughout this work.

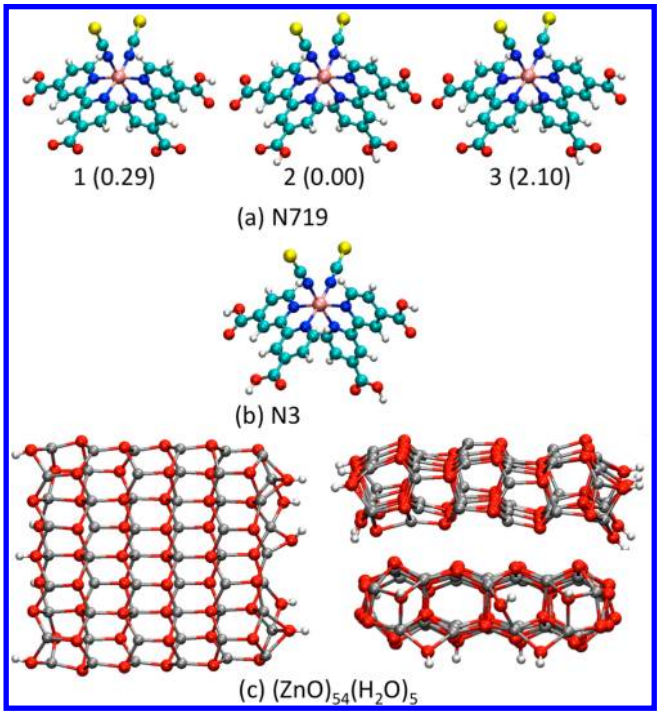

Figure 1. Optimized geometrical structures of the (a) N719, (b) N3, and (c) ZnO models considered in this work. For N719, values in parentheses indicate the relative stability, in kcal/mol, of each isomer with respect to the lowest-lying **2**. For ZnO, views along the $[10\bar{1}0]$ (left), $[11\bar{2}0]$ (right, top), and $[000\bar{1}]$ (right, bottom) axes are provided.

To reproduce the $(10\bar{1}0)$ facets often found in ZnO nanostructures, a $(ZnO)_{54}$ slab has been built up from an underlying wurtzite structure. To minimize the dipole along the [0001] axis and stabilize the cluster, we saturate the polar Zn- and O-terminated surfaces with dissociated water molecules.[48−50] The ZnO model, which has 1.4 × 1.5 nm dimensions along the [1210] × [0001] directions, is large enough to accommodate the N3 and N719 molecules, and it allows us to explore the different adsorption modes of the sensitizers. Regarding the N3 dye, no simplifications were made in its structure. For the N719 dye, however, we did not consider the counterions because their effect on the ground- and excited-state energy levels is predicted to be marginal.[3] As one may notice from Figure 1, three isomers of N719 have

dx.doi.org/10.1021/jp501058x | J. Phys. Chem. A 2014, 118, 5885−5893

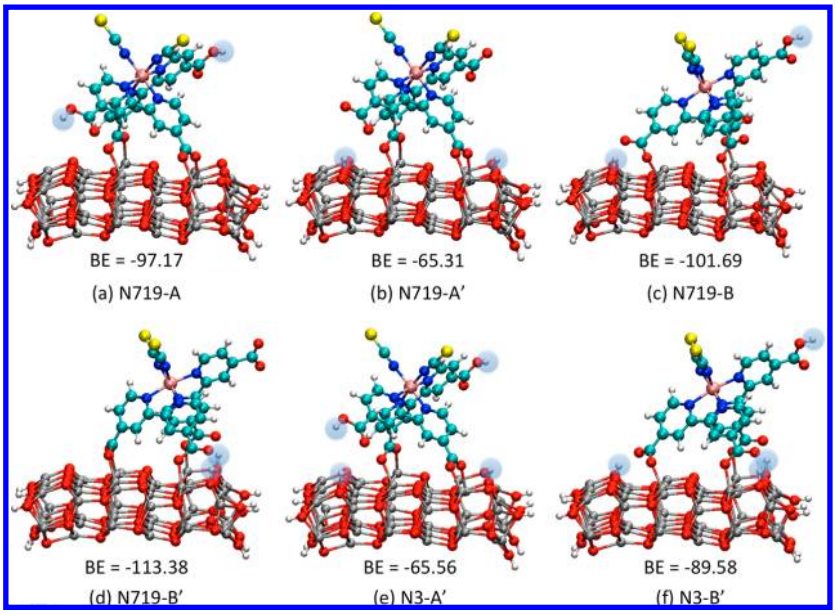

Figure 2. Optimized geometrical structures of the N719@ZnO (a−d) and N3@ZnO (e,f) models considered in this work. Protons are highlighted in blue. BE stands for the binding energy, given in kcal/mol.

been considered, **1** and **2**, where the protonated carboxyls are cis and trans, respectively, to the NCS ligands, and **3**, in which the protonated groups are one in cis and the other in trans. As one may notice from Figure 1, **1** and **2** are almost degenerate in energy, with **3** lying 2.1 kcal/mol higher in energy.[39] Our values are consistent with NMR data, which rule out the existence of isomer **3**.[3] Accordingly, only isomers **1** and **2** have been considered to investigate the adsorption of N719 on ZnO.

All of the models have been fully optimized without any symmetry constraint by means of the BP86[51,52] xc functional within the Kohn−Sham framework of DFT (KS-DFT), as implemented in the ADF 2012.01 software package.[53] A double-ζ basis set (DZ) of Slater-type orbitals (STOs) have been employed. For simplicity, geometry optimizations have been conducted in the gas phase. To characterize the interaction between the dyes and the ZnO surface, we have taken advantage of the bond energy decomposition scheme developed by Ziegler and Rauk[54] and implemented in ADF. Under this scheme, the overall bond energy between two fragments ΔE is broken down in two main terms

$$\Delta E = \Delta E_{\text{prep}} + \Delta E_{\text{int}}$$

The preparation energy ΔE_{prep} accounts for the energy required to deform the separated fragments from their equilibrium structure to their geometry in the complex. The interaction energy ΔE_{int} refers to the instantaneous interaction between the prepared fragments. This term is further decomposed in four contributions, namely, the Pauli repulsion ΔE_{Pauli}, the electrostatic interaction ΔV_{elst}, the orbital interaction ΔE_{oi}, and the dispersion interaction ΔE_{disp}

$$\Delta E_{\text{int}} = \Delta E_{\text{Pauli}} + \Delta V_{\text{elst}} + \Delta E_{\text{oi}} + \Delta E_{\text{disp}}$$

Recall that within this energy decomposition scheme, the attractive and repulsive terms are negative and positive, respectively. Therefore, the more negative the energy term, the more attractive the corresponding interaction.

GGA functionals have shown to properly reproduce the geometries and the energetics of DSSC models, at a fraction of the computational cost required by their hybrid counterparts. However, they severely underestimate the HOMO−LUMO gap of both the dyes and the semiconductor. Therefore, the B3LYP[55] functional has been used, in conjunction with the DGDZVP basis set, to perform the ground- and excited-state TDDFT calculations on the optimized structures. For computational performance, calculations involving B3LYP have been carried out by means of the Gaussian09 package.[56] The effect of water solvation has been included by means of the conductor-like polarizable continuum model (CPCM).[57]

3. RESULTS AND DISCUSSION

3.1. Adsorption Modes. The adsorption of the dye on the semiconductor surface is known to play a crucial role on DSSCs.[39] Indeed, the strength of the dye/semiconductor interaction determines the stability of the nanocomposite lying at the heart of the solar cell. Also, the electronic levels of both the sensitizer and the semiconductor may be modified due to their mutual interaction.

A correct prediction of the adsorption geometry is an essential prerequisite to properly capture the intricate electronic structure of the dye@ZnO nanocomposites. Therefore, different adsorption modes have been studied for the interacting system; see Figure 2.

Regarding N719, we started by placing isomer **1** with the two carboxylate groups facing the ZnO slab (N719-A). Upon optimization, the carboxylate groups adopt a bridging bidentate geometry. A second geometry was also checked, where a third acidic group was allowed to interact with the semiconductor (N719-B). Along the optimization, a proton transfer from this group to a neighboring surface oxygen is observed, suggesting that dissociative adsorption is favored on ZnO surfaces, as found for TiO_2.[37] To check this hypothesis, two additional geometries were considered (N719-A′ and N719-B′) by adsorbing isomer **2** with the protonated carboxylic groups facing the ZnO cluster. As expected, the most stable complexes imply proton transfer to the oxide surface. Note that N719-A′ and N719-B′ closely resemble N719-A and N719-B, with the two acidic protons initially carried by the dye being transferred to the ZnO cluster. This allows us to investigate the dye/ZnO

dx.doi.org/10.1021/jp501058x | J. Phys. Chem. A 2014, 118, 5885−5893

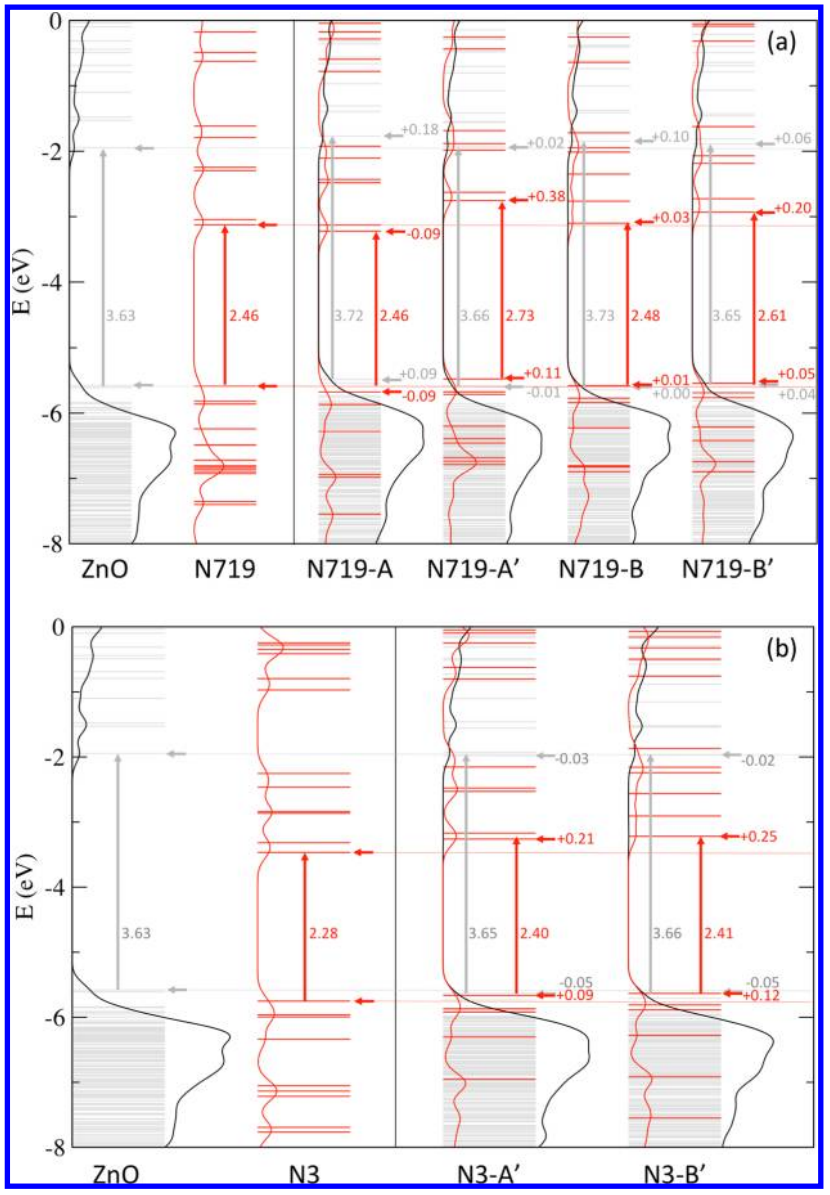

Figure 3. Electronic structure of the (a) N719@ZnO and (b) N3@ZnO models considered in this work (right panels), along with the electronic structure of the isolated fragments (left panels). Red (gray) bars represent the Kohn−Sahm orbitals mostly localized on the sensitizer (ZnO). Horizontal red (gray) arrows highlight the HOMO and LUMO levels of the sensitizer (ZnO). Vertical red (gray) arrows highlight the Kohn−Sham gaps of the sensitizer (ZnO). Red (black) lines represent the density of states, drawn by a Gaussian convolution of σ = 0.20 eV of the individual electronic levels and projected on the sensitizer (ZnO).

protonation effects separately. For the N3@ZnO model, two adsorption modes have been considered, (1) N3-A′, where the dye interacts by means of two of the acidic groups, and (2) N3-B′, where three carboxylic groups are involved in the anchoring of the dye. On the basis of the geometry found for N719-B, dissociative adsorption has been considered for N3-A′ and N3-B′.

The N719 dye is predicted to strongly interact with the ZnO surface, with a computed binding energy of −97.2 kcal/mol for the N719-A model; see Figure 1. The ZnO cluster undergoes an important distortion to enhance the interaction with N719, with a calculated preparation energy of 30.0 kcal/mol. Regarding the dye, the departure from the optimized geometry implies an energy penalty of only 9.1 kcal/mol. The interaction is electrostatically driven, covering 66% of the attractive terms. The importance of the orbital interaction (34%), however, means that the polarization effects are important on the surface of this kind of complexes. Accordingly, a charge donation of ∼0.5 e is found from the dye to the ZnO surface. This charge transfer is expected to modify the electronic structure of both the sensitizer and the semiconductor (vide infra).[58] The N719-B model, where a third acid group interacts with the ZnO slab, lies slightly lower in energy than N719-A, with a calculated binding energy of −101.7 kcal/mol. The N719-A′ geometry is 32 kcal/mol less stable than N719-A. On the other hand, the N719-B′ isomer lies 12 kcal/mol lower than N719-B.

From our results, N719 sticks better on the ZnO surface when three carboxylic groups are involved than when only two of them are exploited. Furthermore, if the anchoring group carries a proton, the adsorption is predicted to be dissociative. Our results are in agreement with previous works on N719-sensitized TiO_2 anatase (101) surfaces.[38,59] In these studies, the

dx.doi.org/10.1021/jp501058x | J. Phys. Chem. A 2014, 118, 5885−5893

configuration where two protons were transferred from the carboxylic groups to the surface was found to lie 37 kcal/mol higher in energy than if the sensitizer was adsorbed exploiting the deprotonated carboxylate groups, and the protons were retained in the dye. From our data, however, N719-A′ is predicted to be energetically unfavorable by 32 kcal/mol.

Regarding the protonated N3 dye, binding energies of −65.5 and −89.6 kcal/mol have been found for N3-A′ and N3-B′. Again, the adsorption by means of three anchoring groups is not only possible but energetically favored by ∼25 kcal/mol.

3.2. Electronic and Optical Properties. We start by investigating the electronic structure of the isolated dyes. As one may notice from Figure 3, for N719 in solution, we find HOMO and LUMO values of −5.59 and −3.13 eV, respectively, in good agreement with reference theoretical results.[38] Regarding the N3 dye, the HOMO is stabilized compared to N719, due to diminished charge donation to the metal, where the high-lying occupied orbitals are mainly localized. The LUMO, localized on the bipyridine ligands bearing the protonated acid groups, is also stabilized but to a larger extent, in such a way that the HOMO−LUMO narrows from N719 (2.47 eV) to N3 (2.28 eV).

Regarding the ZnO model, the calculated band gap of 3.63 eV reasonably compares with the experimental values for ultrasmall ZnO nanoparticles, with reported numbers between 3.4 and 3.8 eV.[23−25] As is evident from Figure 3, however, the valence band edge (VBE) at −5.58 eV essentially coincides with the HOMO levels of N719 and N3, whereas the CBE, at −1.95 eV, lies ∼1.2 eV higher than the LUMO levels of the sensitizers. The band edges are in agreement with our previous results on small ZnO models.[42] Recently, Hedrick et al. found a similar alignment of electronic levels for the magic $(ZnO)_{33}$ nanoparticle sensitized with ruthenium(II) polypyridine molecules.[43] Notably, the dye/semiconductor alignment of energy levels is not correctly reproduced by our models, in particular, the gap between the dye's LUMO and the semiconductor's CBE is probably overestimated in our calculations. The limited size of the model is expected to artificially shift the CBE of ZnO upward.[42] Also, the VBE is too high in energy compared to the dye HOMO, which is placed correctly. This imbalance in dye/semiconductor electronic structure still represents a challenge for current DFT methods.

Having the limitation of our model and computational framework in mind, we mainly focus on the effect of the complexation on the electronic structure of both the dye and the semiconductor, which are expected to be reasonably independent from the employed model. As one may notice from Figure 3, the CBE of ZnO, comprised primarily of Zn 4s states, rises by 0.2 eV in the N719-A complex due to the interaction with the dye. Such an upward shift of the lowest-lying unoccupied states, already reported other II−VI materials and TiO_2,[38,60−63] has been attributed to the electrostatic field induced by the sensitizer and the charge density transferred from the dye to the semiconductor upon the interaction. The VBE of ZnO arising from the O 2p orbitals also rises but to a lesser extent (0.1 eV). As a consequence, the HOMO−LUMO gap of ZnO widens by ∼0.1 eV with respect to the noninteracting cluster. Concomitant with the upward shift of the band edges of ZnO and the opening of the gap is the stabilization of the HOMO level of N719 by 0.1 eV, due to the dye charge transfer to ZnO. The LUMO lowers similarly, and the HOMO−LUMO gap remains unchanged relative to the isolated dye.

Regarding the protonation effects, the electronic structure of N719-A′ reveals that the semiconductor levels are restored when protons are transferred from the dye to the ZnO. Apparently, the charge donation from the dye to the semiconductor is compensated for by the protons adsorbed on the surface of the latter. Regarding the sensitizer, the HOMO level is destabilized because the charge donation from the bipyridine ligands to the Ru metal increases upon deprotonation. The upward shift of the LUMO levels is even larger, in such a way that the HOMO−LUMO gap widens by ∼0.3 eV.

A similar situation is found for the N719-B complex, where N719 exploits three carboxylic groups to sensitize the ZnO surface and a proton has already been transferred to semiconductor. Charge donation from the dye to the semiconductor stabilizes the frontier orbitals of the former, whereas the band edges of the latter rise. The proton transferred to the ZnO slab, however, somehow balances the charge donation effect and recovers the electronic levels of the isolated fragments. Upon a second proton transfer (N719-B′), the dye levels rise, and the ZnO band edges move downward (or remain almost the same), as found for N719-A and N719-A′.

The results found for N3 are consistent with those reported for N719. The band edges of ZnO remain almost constant relative to the isolated cluster. Again, the surface protonation seems to counterbalance the charge density donation from the sensitizer. Regarding the N3 molecule, the HOMO and the LUMO levels rise upon the interaction, but the latter undergoes a larger shift; therefore, the HOMO−LUMO gap opens by ∼0.1 eV. N3-A′ and N3-B′ display similar electronic structures, meaning that the adsorption mode (two versus three anchoring groups) plays a minor role on the electronic structure of the dye@ZnO nanocomposite, as one might anticipate from the data retrieved for N719@ZnO complexes.

Even if the Kohn−Sham molecular orbitals and their eigenvalues may deliver a reasonable picture for the electronic excitation energies of the systems studied here, the accurate description of the excited states requires a more rigorous framework, like the one provided by TDDFT. Figure 4 displays the simulated absorption spectra of the dye@ZnO models considered.

Regarding the isolated fragments, the simulated TDDFT spectra are in line with the experimental data available. As one may notice from Figure 4, the N719 sensitizer displays a lowest energy absorption band at 2.22 eV, in fairly good agreement with the experimental value of 2.35 eV.[3] Regarding N3, we find a single band at 2.52 eV, with a shoulder at 2.05 eV. Experimentally, the lowest-lying absorption band of N3 (in ethanol) appears at 2.30 eV.[64] Regarding ZnO, our model displays a broad feature centered at 3.5 eV, with similarly small ZnO nanoparticles absorbing at 3.4−3.8 eV.[23−25]

As is immediately clear from Figure 4, there is no spectral overlap between the sensitizers and the ZnO, in line with the energy levels mismatch discussed above. As a consequence, the lowest-lying electronic excitations of the interacting complexes are mainly localized on the dye. Accordingly, the simulated absorption spectra of the dye@ZnO models closely resemble the optical spectra of the isolated dyes. In this respect, our results may resemble those obtained with an embedding scheme in which the semiconductor only produces a perturbation on the dye energy levels. Similar results were recently reported for the $(ZnO)_{33}$ nanoparticle sensitized with

dx.doi.org/10.1021/jp501058x | J. Phys. Chem. A 2014, 118, 5885−5893

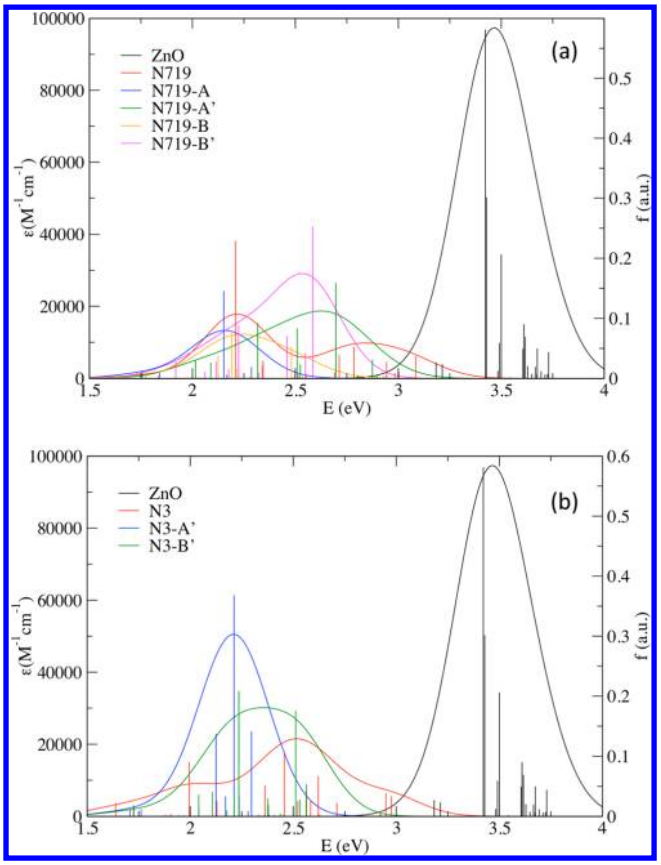

Figure 4. TDDFT absorption spectra of the (a) N719@ZnO and (b) N3@ZnO models considered in this work, obtained by a Gaussian convolution with fwhm = 0.37 eV, calculated taking into account the 20 lowest singlet−singlet electronic transitions. For comparison, the spectra of the isolated dyes/ZnO are also shown.

Ru(II) polypyridine ligands, with the first band at 2.7−3.2 eV belonging to the dye transitions.[43]

To better characterize the lowest-lying transitions, their associated charge density differences have been computed. In Figure 5, the electron density difference maps (EDDMs) related to the first and the brightest excitations are collected. As one may notice from Figure 5, the electron localizes on the dye's bipyridine ligands, irrespective of the sensitizer and the adsorption mode. In fact, as already discussed above, the LUMOs of both N719 and N3 lie below the CBE of the employed ZnO models. Accordingly, there is no admixture of the dye/ZnO states in the lowest-lying unoccupied states of the interacting complexes.[42] The hole localizes on the Ru center and the NCS ligands, but often, there is a sizable contribution from the semiconductor. From Figure 5, it seems that the hole localization on the ZnO cluster is favored when the sensitizer exploits three carboxylic groups to anchor the semiconductor surface. We notice, however, that this is an unphysical situation, which is driven by the improper alignment of energy levels.

4. SUMMARY AND CONCLUSIONS

Recently, ZnO has earned a lot of attention as an interesting alternative to TiO_2 for DSSCs due to a better electron mobility and a fascinating structural diversity. However, ZnO-based devices have worked quite dissapointingly so far, and the reasons underneath remain unclear. Here, we have presented a DFT/TDDFT study on the interaction between the prototypical Ru(II) bypyridyl sensitizers N3/N719 and ZnO, aimed to understand some of the atomistic details governing the performance of DSSCs. We have explored different adsorption modes for the sensitizers because a correct prediction of the interacting geometry is an essential prerequisite to properly reproduce the complex electronic structure of dye@ZnO compounds. Then, we investigated the effect of the complexation on the electronic structure of the sensitizers and the semiconductor.

From our results, N719 adsorbs better on the ZnO surface when three carboxylic groups are exploited than when only two are involved. Moreover, if the anchoring group bears a proton, the adsorption is predicted to be dissociative. On the contrary,

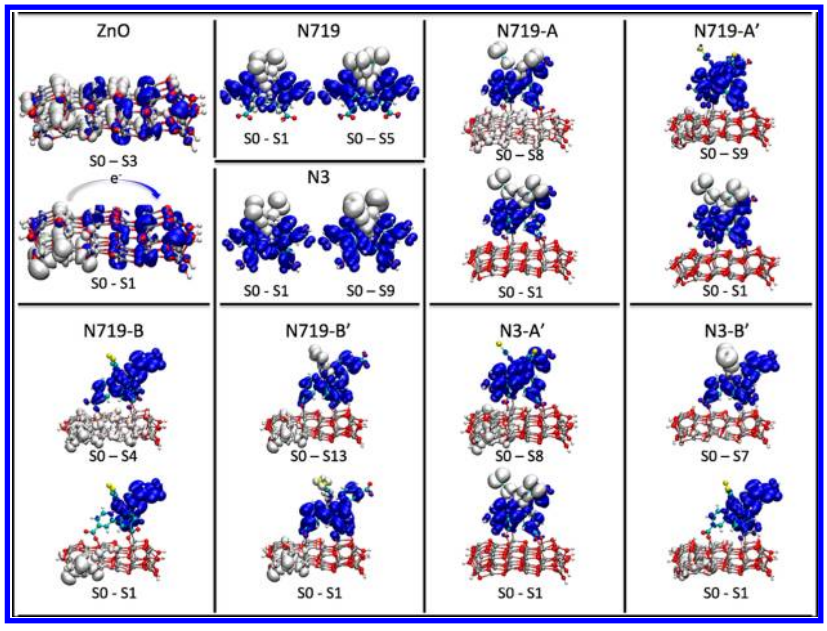

Figure 5. Selected EDDMs of the singlet−singlet electronic transitions for the N719@ZnO N3@ZnO models considered in this work. For comparison, the EDDMs of the isolated dyes/ZnO are also shown. Isocontour value of 0.0002 au.

dx.doi.org/10.1021/jp501058x | J. Phys. Chem. A 2014, 118, 5885−5893

proton transfer from distal carboxylic moieties to the ZnO surface is energetically unfavorable. The interaction is mainly electrostatic, covering 2/3 of the attractive terms. Nevertheless, the orbital contribution is also sizable, meaning that the polarization effects on the semiconductor surface are also important. N3 shows a slightly weaker affinity than N719 toward the ZnO nanoparticle, but the interaction is still strong enough (∼−66 kcal/mol) to ensure an stable anchoring of the dye.

We have found the sensitizers' LUMOs to lie ∼1.2 eV below the CBE of the ZnO nanoparticle. This unphysical alignment of electronic levels is due to two combined effects, that is, the reduced size of the considered ZnO cluster and to some extent to a nonoptimal description of the ZnO energy levels by standard DFT functionals. On the contrary, the dye energy levels are nicely accounted for by standard DFT. Despite these model limitations, the considered systems allowed us to qualitatively evaluate the effect of the interaction on the electronic structure of the sensitizer and the semiconductor.

If the acidic protons are retained on the dye, the adsorption of the sensitizer raises the CBE of the ZnO due to the electrostatic field induced by the Ru(II) complex and the charge density transferred to the semiconductor. The VBE also rises but to a lesser extent; therefore, the semiconductor gap widens. Proton transfer from the dye to the semiconductor balances the charge donation effects and restores the electronic levels of the noninteracting fragments. The adsorption mode (two versus three anchoring groups) seems to play a minor role on the electronic structure of the dye@ZnO complex.

The TDDFT calculations reveal that the sensitizer's optical features appear at 1.5−3.5 eV, with the ZnO model absorbing at 3.0−4.0 eV. Due to the small spectral overlap between the sensitizers and the semiconductor, the lowest-lying electronic excitations of the interacting complexes are mainly localized on the dyes. The photoexcited electrons are predicted to localize on the bipyridine ligands, with negligible contribution from the ZnO states.

This study confirms the difficulty of simulating ZnO/dye interactions in a proper theoretical framework, that is, including a TDDFT description of the excited states of the joint system along with the effect of a surrounding solvation. Probably, post-DFT methods will be needed to encompass such difficulty.

■ ASSOCIATED CONTENT

Supporting Information

Complete author list of ref 56. This material is available free of charge via the Internet at http://pubs.acs.org.

■ AUTHOR INFORMATION

Corresponding Author

*E-mail:filippo@thch.unipg.it. Telephone: +390755855522.

Notes

The authors declare no competing financial interest.

■ ACKNOWLEDGMENTS

This research was funded by Eusko Jaurlaritza/Basque Government (IT588-13 and S-PC12UN003) and the Spanish Office for Scientific Research (CTQ2012-38496-C05-01). The SGI/IZO-SGIker UPV/EHU is gratefully acknowledged for generous allocation of computational resources. J.M.A. would like to thank the Spanish Ministry of Education for funding through a FPU fellowship (AP2009-1514). F.D.A. thanks FP7-ENERGY-2010 project "ESCORT"(261920) and CNR-EFOR for financial support.

■ REFERENCES

(1) O'Regan, B.; Grätzel, M. A Low-Cost, High-Efficiency Solar Cell Based on Dye-Sensitized Colloidal TiO_2 Films. *Nature* **1991**, *353*, 737−740.

(2) Pastore, M.; Fantacci, S.; De Angelis, F. Modeling Excited States and Alignment of Energy Levels in Dye-Sensitized Solar Cells: Successes, Failures, and Challenges. *J. Phys. Chem. C* **2013**, *117*, 3685−3700.

(3) Nazeeruddin, M. K.; De Angelis, F.; Fantacci, S.; Selloni, A.; Viscardi, G.; Liska, P.; Ito, S.; Takeru, B.; Grätzel, M. Combined Experimental and DFT-TDDFT Computational Study of Photoelectrochemical Cell Tuthenium Sensitizers. *J. Am. Chem. Soc.* **2005**, *127*, 16835−16847.

(4) Nazeeruddin, M. K.; Kay, A.; Rodicio, I.; Humphry-Baker, R.; Mueller, E.; Liska, P.; Vlachopoulos, N.; Gratzel, M. Conversion of Light to Electricity by *cis*-X_2Bis(2,2′-bipyridyl-4,4′-dicarboxylate)-ruthenium(II) charge-transfer sensitizers (X = Cl^-, Br^-, I^-, CN^-, and SCN^-) on Nanocrystalline TiO_2 Electrodes. *J. Am. Chem. Soc.* **1993**, *115*, 6382−6390.

(5) De Angelis, F.; Fantacci, S.; Mosconi, E.; Nazeeruddin, M. K.; Grätzel, M. Absorption Spectra and Excited State Energy Levels of the N719 Dye on TiO_2 in Dye-Sensitized Solar Cell Models. *J. Phys. Chem. C* **2011**, *115*, 8825−8831.

(6) Tiwana, P.; Docampo, P.; Johnston, M. B.; Snaith, H. J.; Herz, L. M. Electron Mobility and Injection Dynamics in Mesoporous ZnO, SnO_2, and TiO_2 Films Used in Dye-Sensitized Solar Cells. *ACS Nano* **2011**, *5*, 5158−5166.

(7) Grätzel, M. Photoelectrochemical Cells. *Nature* **2001**, *414*, 338−344.

(8) Katoh, R.; Furube, A.; Yoshihara, T.; Hara, K.; Fujihashi, G.; Takano, S.; Murata, S.; Arakawa, H.; Tachiya, M. Efficiencies of Electron Injection from Excited N3 Dye into Nanocrystalline Semiconductor (ZrO_2, TiO_2, ZnO, Nb_2O_5, SnO_2, In_2O_3) Films. *J. Phys. Chem. B* **2004**, *108*, 4818−4822.

(9) Asbury, J. B.; Hao, E.; Wang, Y.; Ghosh, H. N.; Lian, T.; V, E. U. Ultrafast Electron Transfer Dynamics from Molecular Adsorbates to Semiconductor. *J. Phys. Chem. B* **2001**, *105*, 4545−4557.

(10) Fessenden, R. W.; Kamat, P. V. Rate Constants for Charge Injection from Excited Sensitizer into SnO_2, ZnO, and TiO_2 Semiconductor Nanocrystallites. *J. Phys. Chem.* **1995**, *99*, 12902−12906.

(11) Fukai, Y.; Kondo, Y.; Mori, S.; Suzuki, E. Highly Efficient Dye-Sensitized SnO_2 Solar Cells Having Sufficient Electron Diffusion Length. *Electrochem. Commun.* **2007**, *9*, 1439−1443.

(12) Look, D. C.; Reynolds, D. C.; Sizelove, J. R.; Jones, R. L.; Litton, C. W.; Cantwell, G.; Harsh, W. C. Electrical Properties of Bulk ZnO. *Solid State Commun.* **1998**, *105*, 399−401.

(13) Jarzebski, Z. M.; Marton, J. P. Physical Properties of SnO_2 Materials. *J. Electrochem. Soc.* **1976**, *123*, 299−310.

(14) Jousse, D.; Constantino, C.; Chambouleyron, I. Highly Conductive and Transparent Amorphous Tin Oxide. *J. Appl. Phys.* **1983**, *54*, 431−434.

(15) Shanthi, E.; Dutta, V.; Banerjee, A.; Chopra, K. L. Electrical and Optical Properties of Undoped and Antimony-Doped Tin Oxide Films. *J. Appl. Phys.* **1980**, *51*, 6243−6251.

(16) Djurisic, A. B.; Leung, Y. H. Optical Properties of ZnO Nanostructures. *Small* **2006**, *2*, 944−961.

(17) Fang, X.; Bando, Y.; Gautam, U. K.; Zhai, T.; Zeng, H.; Xu, X.; Liao, M.; Golberg, D. ZnO and ZnS Nanostructures: Ultraviolet-Light Emitters, Lasers, and Sensors. *Crit. Rev. Solid State Mater. Sci.* **2009**, *34*, 190−223.

(18) Law, M.; Greene, L. E.; Johnson, J. C.; Saykally, R.; Yang, P. Nanowire Dye-Sensitized Solar Cells. *Nat. Mater.* **2005**, *4*, 455−459.

(19) Memarian, N.; Concina, I.; Braga, A.; Rozati, S. M.; Vomiero, A.; Sberveglieri, G. Hierarchically Assembled ZnO Nanocrystallites for

High-Efficiency Dye-Sensitized Solar Cells. *Angew. Chem., Int. Ed.* **2011**, *123*, 12529−12533.
(20) Yella, A.; Lee, H.-W.; Tsao, H. N.; Yi, C.; Chandiran, A. K.; Nazeeruddin, M. K.; Diau, E. W.-G.; Yeh, C.-Y.; Zakeeruddin, S. M.; Grätzel, M. Porphyrin-Sensitized Solar Cells with Cobalt(II/III)-Based Redox Electrolyte Exceed 12% Efficiency. *Science* **2011**, *334*, 629−634.
(21) Szarko, J. M.; Neubauer, A.; Bartelt, A.; Socaciu-siebert, L.; Birkner, F.; Schwarzburg, K.; Hannappel, T.; Eichberger, R. The Ultrafast Temporal and Spectral Characterization of Electron Injection from Perylene Derivatives into ZnO and TiO_2 Colloidal Films. *J. Phys. Chem. C* **2008**, *112*, 10542−10552.
(22) Moser, J.-E. Dynamics of Interfacial and Surface Electron Transfer Processes. In *Dye-Sensitized Solar Cells*; Kalyanasundaram, K., Ed.; EPFL Press: Laussane, Switzerland, 2010; pp 403−456.
(23) Monticone, S.; Tufeu, R.; Kanaev, A. V. Complex Nature of the UV and Visible Fluorescence of Colloidal ZnO Nanoparticles. *J. Phys. Chem. B* **1998**, *102*, 2854−2862.
(24) van Dijken, A.; Meulenkamp, E. A.; Vanmaekelbergh, D.; Meijerink, A. The Kinetics of the Radiative and Nonradiative Processes in Nanocrystalline ZnO Particles upon Photoexcitation. *J. Phys. Chem. B* **2000**, *104*, 1715−1723.
(25) Kahn, M. L.; Cardinal, T.; Bousquet, B.; Monge, M.; Jubera, V.; Chaudret, B. Optical Properties of Zinc Oxide Nanoparticles and Nanorods Synthesized Using an Organometallic Method. *ChemPhysChem* **2006**, *7*, 2392−2397.
(26) Viswanatha, R.; Sapra, S.; Satpati, B.; Satyam, P. V.; Dev, B. N.; Sarma, D. D. Understanding the Quantum Size Effects in ZnO Nanocrystals. *J. Mater. Chem.* **2004**, *14*, 661−668.
(27) Guillén, E.; Azaceta, E.; Peter, L. M.; Zukal, A.; Tena-Zaera, R.; Anta, J. a. ZnO Solar Cells with an Indoline Sensitizer: A Comparison between Nanoparticulate Films and Electrodeposited Nanowire Arrays. *Energy Environ. Sci.* **2011**, *4*, 3400−3407.
(28) Anta, J. A.; Guillén, E.; Tena-Zaera, R. ZnO-Based Dye-Sensitized Solar Cells. *J. Phys. Chem. C* **2012**, *116*, 11413−11425.
(29) Asbury, J. B.; Wang, Y.; Lian, T.; V, E. U. Multiple-Exponential Electron Injection in $Ru(dcbpy)_2(SCN)_2$ Sensitized ZnO Nanocrystalline Thin Films. *J. Phys. Chem. B* **1999**, *103*, 6643−6647.
(30) Furube, A.; Katoh, R.; Hara, K.; Murata, S.; Arakawa, H.; Tachiya, M. Ultrafast Stepwise Electron Injection from Photoexcited Ru-Complex into Nanocrystalline ZnO Film via Intermediates at the Surface. *J. Phys. Chem. B* **2003**, *107*, 4162−4166.
(31) Furube, A.; Katoh, R.; Yoshihara, T.; Hara, K.; Murata, S.; Arakawa, H.; Tachiya, M. Ultrafast Direct and Indirect Electron-Injection Processes in a Photoexcited Dye-Sensitized Nanocrystalline Zinc Oxide Film: The Importance of Exciplex Intermediates at the Surface. *J. Phys. Chem. B* **2004**, *108*, 12583−12592.
(32) Stockwell, D.; Yang, Y.; Huang, J.; Anfuso, C.; Huang, Z.; Lian, T. Comparison of Electron-Transfer Dynamics from Coumarin 343 to TiO_2, SnO_2, and ZnO Nanocrystalline Thin Films: Role of Interface-Bound Charge-Separated Pairs. *J. Phys. Chem. C* **2010**, *114*, 6560−6566.
(33) Oskam, G.; Hu, Z.; Penn, R.; Pesika, N.; Searson, P. Coarsening of Metal Oxide Nanoparticles. *Phys. Rev. E* **2002**, *66*, 011403/1−011403/4.
(34) Nguyen, H.-M.; Mane, R. S.; Ganesh, T.; Han, S.-H.; Kim, N. Aggregation-Free ZnO Nanocrystals Coupled HMP-2 Dye of Higher Extinction Coefficient for Enhancing Energy Conversion Efficiency. *J. Phys. Chem. C* **2009**, *113*, 9206−9209.
(35) González-Moreno, R. n.; Cook, P. L.; Zegkinoglou, I.; Liu, X.; Johnson, P. S.; Yang, W.; Ruther, R. E.; Hamers, R. J.; Tena-Zaera, R. n.; Himpsel, F. J.; Ortega, J. E.; Rogero, C. Attachment of Protoporphyrin Dyes to Nanostructured ZnO Surfaces: Characterization by Near Edge X-ray Absorption Fine Structure Spectroscopy. *J. Phys. Chem. C* **2011**, *115*, 18195−18201.
(36) Guillén, E.; Idígoras, J.; Berger, T.; Anta, J. a.; Fernández-Lorenzo, C.; Alcántara, R.; Navas, J.; Martín-Calleja, J. ZnO-Based Dye Solar Cell with Pure Ionic-Liquid Electrolyte and Organic Sensitizer: The Relevance of the Dye−Oxide Interaction in an Ionic-Liquid Medium. *Phys. Chem. Chem. Phys.* **2011**, *13*, 207−213.
(37) Anselmi, C.; Mosconi, E.; Pastore, M.; Ronca, E.; De Angelis, F. Adsorption of Organic Dyes on TiO_2 Surfaces in Dye-Sensitized Solar Cells: Interplay of Theory and Experiment. *Phys. Chem. Chem. Phys.* **2012**, *14*, 15963−15974.
(38) De Angelis, F.; Fantacci, S.; Selloni, A. Alignment of the Dye's Molecular Levels with the TiO_2 Band Edges in Dye-Sensitized Solar Cells: A DFT-TDDFT Study. *Nanotechnology* **2008**, *19*, 424002(1−7).
(39) De Angelis, F.; Fantacci, S.; Selloni, A.; Grätzel, M.; Nazeeruddin, M. K. Influence of the Sensitizer Adsorption Mode on the Open-Circuit Potential of Dye-Sensitized Solar Cells. *Nano Lett.* **2007**, *7*, 3189−3195.
(40) De Angelis, F.; Fantacci, S.; Selloni, A.; Nazeeruddin, M. K.; Grätzel, M. Time-Dependent Density Functional Theory Investigations on the Excited States of Ru(II)-Dye-Sensitized TiO_2 Nanoparticles: The Role of Sensitizer Protonation. *J. Am. Chem. Soc.* **2007**, *129*, 14156−14157.
(41) Pastore, M.; De Angelis, F. Computational Modelling of TiO_2 Surfaces Sensitized by Organic Dyes with Different Anchoring Groups: Adsorption Modes, Electronic Structure and Implication for Electron Injection/Recombination. *Phys. Chem. Chem. Phys.* **2012**, *14*, 920−928.
(42) Amat, A.; De Angelis, F. Challenges in the Simulation of Dye-Sensitized ZnO Solar Cells: Quantum Confinement, Alignment of Energy Levels and Excited State Nature at the Dye/Semiconductor Interface. *Phys. Chem. Chem. Phys.* **2012**, *14*, 10662−10668.
(43) Hedrick, M. M.; Mayo, M. L.; Badaeva, E.; Kilina, S. First-Principles Studies of the Ground- and Excited-State Properties of Quantum Dots Functionalized by Ru(II)-Polybipyridine. *J. Phys. Chem. C* **2013**, *117*, 18216−18224.
(44) Labat, F.; Ciofini, I.; Adamo, C. Modeling ZnO Phases Using a Periodic Approach: From Bulk to Surface and Beyond. *J. Chem. Phys.* **2009**, *131*, 044708/1−044708/11.
(45) Labat, F.; Ciofini, I.; Hratchian, H. P.; Frisch, M.; Raghavachari, K.; Adamo, C. First Principles Modeling of Eosin-Loaded ZnO Films: A Step Toward the Understanding of Dye-Sensitized Solar Cell Performances. *J. Am. Chem. Soc.* **2009**, *131*, 14290−14298.
(46) Persson, P.; Lunell, S.; Ojamäe, L. Quantum Chemical Prediction of the Adsorption Conformations and Dynamics at HCOOH-Covered ZnO(1010) Surfaces. *Int. J. Quantum Chem.* **2002**, *89*, 172−180.
(47) Persson, P.; Ojamäe, L. Periodic Hartree−Fock Study of the Adsorption of Formic Acid on ZnO (1010). *Chem. Phys. Lett.* **2000**, *231*, 302−308.
(48) De Angelis, F.; Armelao, L. Optical Properties of ZnO Nanostructures: A Hybrid DFT/TDDFT Investigation. *Phys. Chem. Chem. Phys.* **2011**, *13*, 467−475.
(49) Azpiroz, J. M.; Infante, I.; Lopez, X.; Ugalde, J. M.; De Angelis, F. A First-Principles Study of II−VI (II = Zn; VI = O, S, Se, Te) Semiconductor Nanostructures. *J. Mater. Chem.* **2012**, *22*, 21453−21465.
(50) Azpiroz, J. M.; Mosconi, E.; De Angelis, F. Modeling ZnS and ZnO Nanostructures: Structural, Electronic, and Optical Properties. *J. Phys. Chem. C* **2011**, *115*, 25219−25226.
(51) Becke, A. D. Correlation Energy of an Inhomogeneous Electron Gas: A Coordinate-Space Model. *J. Chem. Phys.* **1988**, *88*, 1053.
(52) Perdew, J. P. Density-Functional Approximation for the Correlation Energy of the Inhomogeneous Electron Gas. *Phys. Rev. B* **1986**, *33*, 8822−8824.
(53) Velde, G. T.; Bickelhaupt, F. M.; Baerends, E. J.; Guerra, C. F.; Gisbergen, S. J. A. V.; Snijders, J. G.; Ziegler, T. Chemistry with ADF. *J. Comput. Chem.* **2001**, *22*, 931−967.
(54) Ziegler, T.; Rauk, A. On the Calculation of Bonding Energies by the Hartree Fock Slater Method. I. The Transition State Method. *Theor. Chim. Acta* **1977**, *46*, 1−10.
(55) Becke, A. D. Density-Functional Thermochemistry. III. The Role of Exact Exchange. *J. Chem. Phys.* **1993**, *98*, 5648−5652.
(56) Frisch, M. J.; Trucks, G. W.; Schlegel, H. B.; Scuseria, G. E.; Robb, M. A.; Cheeseman, J. R.; Scalmani, G.; Barone, V.; Mennucci,

B.; Petersson; et al. *Gaussian 09*, revision B.01; Gaussian Inc.: Wallingford, CT, 2009.
(57) Cossi, M.; Rega, N.; Scalmani, G.; Barone, V. Energies, Structures, and Electronic Properties of Molecules in Solution with the C-PCM Solvation Model. *J. Comput. Chem.* **2003**, *24*, 669−681.
(58) Ronca, E.; Pastore, M.; Belpassi, L.; Tarantelli, F.; De Angelis, F. Influence of the Dye Molecular Structure on the TiO_2 Conduction Band in Dye-Sensitized Solar Cells: Disentangling Charge Transfer and Electrostatic Effects. *Energy Environ. Sci.* **2013**, *6*, 183−193.
(59) De Angelis, F.; Fantacci, S.; Selloni, A.; Nazeeruddin, M. K.; Gra, M. First-Principles Modeling of the Adsorption Geometry and Electronic Structure of Ru(II) Dyes on Extended TiO_2 Substrates for Dye-Sensitized Solar Cell Applications. *J. Phys. Chem. C* **2010**, *114*, 6054−6061.
(60) Bahers, T. L.; Labat, F.; Pauporté, T.; Lainé, P. P.; Ciofini, I. Theoretical Procedure for Optimizing Dye-Sensitized Solar Cells: From Electronic Structure to Photovoltaic Efficiency. *J. Am. Chem. Soc.* **2011**, *133*, 8005−8013.
(61) Zwijnenburg, M. A.; Illas, F.; Bromley, S. T. The Fate of Optical Excitations in Small Hydrated ZnS Clusters: A Theoretical Study into the Effect of Hydration on the Excitation and Localisation of Electrons in Zn_4S_4 and Zn_6S_6. *Phys. Chem. Chem. Phys.* **2011**, *13*, 9311−9317.
(62) Zwijnenburg, M. A. Photoluminescence in Semiconductor Nanoparticles: An Atomistic View of Excited State Relaxation in Nanosized ZnS. *Nanoscale* **2012**, *4*, 3711−3717.
(63) Azpiroz, J. M.; Matxain, J. M.; Infante, I.; Lopez, X.; Ugalde, J. M. A DFT/TDDFT Study on the Optoelectronic Properties of the Amine-Capped Magic $(CdSe)_{13}$ Nanocluster. *Phys. Chem. Chem. Phys.* **2013**, *15*, 10996−11005.
(64) Fantacci, S.; De Angelis, F.; Selloni, A. Absorption Spectrum and Solvatochromism of the $[Ru(4,4'\text{-}COOH\text{-}2,2'\text{-}bpy)_2(NCS)_2]$ Molecular Dye by Time Dependent Density Functional Theory. *J. Am. Chem. Soc.* **2003**, *125*, 4381−4387.